Force microscopy of layering and friction in an ionic liquid

Judith Hoth[a,b], Florian Hausen[a,1], Martin H. Müser[c], and Roland Bennewitz[a,b]

[a] INM – Leibniz Institute for New Materials, Nanotribology group, Saarbrücken, Germany

[b] Department of Physics, Saarland University, Saarbrücken, Germany

[c] Jülich Supercomputing Centre, Institute for Advanced Simulation, FZ Jülich, Jülich, Germany

Email: roland.bennewitz@inm-gmbh.de

Abstract. The mechanical properties of the ionic liquid 1-butyl-1-methylpyrrolidinium tris(pentafluoroethyl) trifluorophosphate ([$Py_{1,4}$][FAP]) in confinement between a SiO_x and a Au(111) surface are investigated by means of atomic force microscopy (AFM) under electrochemical control. Up to twelve layers of ion pairs can be detected through force measurements while approaching the tip of the AFM to the surface. The particular shape of the force vs. distance curve is explained by a model for the interaction between tip, gold surface, and ionic liquid which assumes an exponentially decaying oscillatory force originating from bulk liquid density correlations. Jumps in the tip-sample distance upon approach correspond to jumps of the compliant force sensor between branches of the oscillatory force curve. Frictional force between the laterally moving tip and the surface is detected only after partial penetration of the last double layer between tip and surface.

Introduction

Room-temperature molten salts, also known as ionic liquids show remarkable properties: negligible vapour pressure, non-flammability, thermal stability, and high electrical conductivity. Due to the variety of possible combinations of anions and cations, it is possible to tailor the just-mentioned and other properties of ionic liquids. This makes them promising candidates for a wide field of applications. One example, relevant to our work, is their potential to serve as a low-viscosity, yet load-bearing lubricant [1-4]. The load-bearing ability stems from the formation of solvation layers that are strongly bound to a solid surface [5]. As such, they can act as a protective and sacrificial layer in a rubbing contact, in which lost material can get replenished quasi-instantly from the bulk fluid. At the same time, low viscosity can be maintained, even at relatively large loads, due to a structural incompatibility of anions and cations. Thus, an ionic liquid may satisfy requirements for lubricants from the hydrodynamic to the boundary lubrication regime.

The interest in the molecular mechanisms of layering and in the shear strength of ionic liquids in nanometer confinement has recently led to a number of experimental and theoretical studies. The distance between the layers close to confining walls corresponds to an ion pair size as confirmed experimentally for a variety of different ionic liquids in force sensitive measurements by means of atomic force microscopy (AFM) [6-10] and surface force apparatus (SFA) [11-13]. Werzer et al. [14]

[1] Current affiliation: Department of Chemistry, University of Oxford, UK

analysed the friction response as a function of the number of ion pair layers of ethylammonium nitrate (EAN) between mica and a silica colloidal AFM probe. The authors found increasing friction for a decreasing number of confined layers. Similar experiments were performed by Smith et al. [15] by means of SFA analysing the friction forces in $[Py_{1,4}][Tf_2N]$ confined between two mica surfaces. Distinct friction regimes corresponding to nine to three ion pairs in the contact were observed, resulting in multiple possible friction values for the same applied normal load. Although one expects the mica surfaces used in these studies to be charged, no direct control or characterisation of surface charges were provided. Sweeney et al. [16] reported on the tribological properties of an ionic liquid at an electrochemically controlled gold surface at different potentials. By varying the potential they found that the potential-dependent layering behaviour of $[Py_{1,4}]$[FAP] leads to lower friction at negative potentials. The authors concluded that the lubrication effect is due to an enriched cation layer with lubricating properties at the glide plane. The importance of cation alkyl chains for the lubricating properties was recently confirmed in a study on imidazolium-based ionic liquids by Li et al. [17].

The interface between ionic liquids and solid surfaces has also been subject of modelling studies. Lanning and Madden [18] found oscillatory forces in molten KCl and suggested that the results also apply to low-temperature molten salts like ionic liquids. Strong layering was found for [DMIM][Cl] confined between parallel walls in a molecular dynamics study by Pinilla et al. [19]. Looking at the influence of different charge densities Kirchner et al. found multi-layered structures in ionic liquids confined between oppositely charged walls [20]. The authors report on a transition from a long-range multi-layered structure to only one ordered layer of counter ions next to the surface for certain charge densities. Merlet et al. recently summarised the results of molecular dynamics and Monte-Carlo simulations of ionic liquids in contact with electrodes of different shape [21].

Despite the often observed formation of a certain number of solvation layers, relatively little is known about the factors influencing these layers and their characteristics. Hayes et al. [7] found that the number of observed layers decreases from seven to four when the temperature is increased from 14°C to 30°C. At the same time the forces required to rupture through each of the layers decreases with increased temperature. The authors attributed this effect to a weakened liquid structuring due to an increased thermal motion of ions. Ueno et al. [22] reported on a correlation between the capability to form strong interactions in the bulk ionic liquid and the structuring in confinement.

Atkin and co-workers [6] described that the orientation of the cation with respect to the surface determines how pronounced the layers are. The authors found that a parallel orientation of the cationic ring structure is favourable for the formation of solvation layers and thus concluded that the roughness of the substrate and the surface charge must play a role. This was confirmed by Li et al. [9] who controlled the potential of a gold electrode and found more pronounced interfacial structures for increased potentials. A surface force apparatus study by Bou-Malham [11] also reported about the significance of surface charges and the type of liquid on the formation of solvation layers. The authors compared the layering capability of two immidazolium-based ionic liquids and the apolar liquid octamethylcyclotetrasiloxane (OMCTS) confined between two charged mica surfaces or two methyl-terminated self-assembled monolayer (SAM) covered mica surface. Solvation layers for the ionic liquid have been only observed in the case of charged substrates while similar layers for OMCTS are not affected by coverage of the surface with a SAM.

The goal of the study described here is to detect friction for a nanometer-scale AFM probe while approaching a gold surface in an ionic liquid showing very pronounced layering. The study is motivated by corresponding results reported for experiments performed using a Surface Forces Apparatus [15]. We show examples for pronounced layering and analyze jumps in the tip-sample

distance by means of a correlation model for the tip-liquid-surface interaction in order to quantify the load-bearing capacity of the layered ionic liquid.

Experiment

Forces acting on the tip of an AFM have been measured while approaching the tip to an Au(111) surface in an ionic liquid. The normal and lateral forces cause flexural and torsional bending of a micro-fabricated cantilever carrying the tip. The bending is detected as deflection of a light beam reflected from the backside of the cantilever by means of a four-segment photodiode. In a perfectly aligned setup, the measurement of normal and lateral forces is decoupled. The realistically achievable alignment of light beam, cantilever, and position-sensitive photodiode leads to a cross-talk between the two signals, mostly of the stronger normal force signal into the lateral force signal. A correction for cross-talk is described for our results below.

All measurements were performed at room temperature with an Agilent 5500 AFM using rectangular Silicon cantilevers (Nanosensors PPP-Cont) with nominal normal spring constants of 0.1 N/m and lateral spring constants of 40 N/m. Prior to experiments, each cantilever was calibrated using the beam geometry method where the thickness of the cantilever was determined from its first resonance frequency [23].

The ultrapure ionic liquid 1-butyl-1-methylpyrrolidinium tris(pentafluoroethyl) trifluorophosphate ([$Py_{1,4}$][FAP], custom synthesis by Merck, Germany, all impurities below 10 ppm) was probed in contact with an Au(111) single crystal surface (MaTecK, Germany). Before each experiment, the crystal was prepared by annealing in a butane flame for 1 min and cooling to room temperature for 2 hours. The setup also comprises a home-built electrochemical cell. The Au(111) crystal constituted the working electrode, the counter electrode was a gold wire and a Pt wire was employed as reference electrode. All potentials in this report are quoted with respect to Pt.

The force vs. distance curves are measured by recording the normal deflection of the cantilever while approaching the cantilever to the sample surface. For some measurements, the force data is recorded in high temporal resolution (transient recorder LTT24 by Tasler Labortechnik, Würzburg, Germany, 4 MHz sampling rate at 24 bit resolution of 10 V signal amplitude). Unfortunately, the control software of the AFM does not allow one to move the tip laterally during these approach experiments. Therefore, we had to implement a work-around for friction experiments at decreasing distances. We start to record friction forces in the normal scanning mode of AFM at a distance of several nanometers from the surface. At time t=0 the set point of the distance controller is set to a certain force known to result in an approach of the tip to the surface. The feedback parameters are chosen very low so that the tip moves slowly towards the surface, the set point is reached only after 5.5 seconds. In this way, changes in the lateral force can be recorded while the tip approaches the surfaces through an ionic liquid layer of decreasing thickness.

Results

Force microscopy of layering

The layering of the ionic liquid [$Py_{1,4}$][FAP] in front of the Au(111) surface at an electrochemical potential of -2V manifests itself in sudden jumps of the tip towards to surface while the repulsive force is continuously increasing during approach. A typical result is shown in figure 1(a). We attribute these jumps to an oscillatory force caused by correlation effects in the confined liquid between tip apex and surface. The experimental result has been reported for several systems of surface and ionic liquid [6-8, 10, 17]. Upon retraction, the tip remains at the same distance from the surface for negative forces up to -1.4 nN, resulting in a significant adhesion hysteresis.

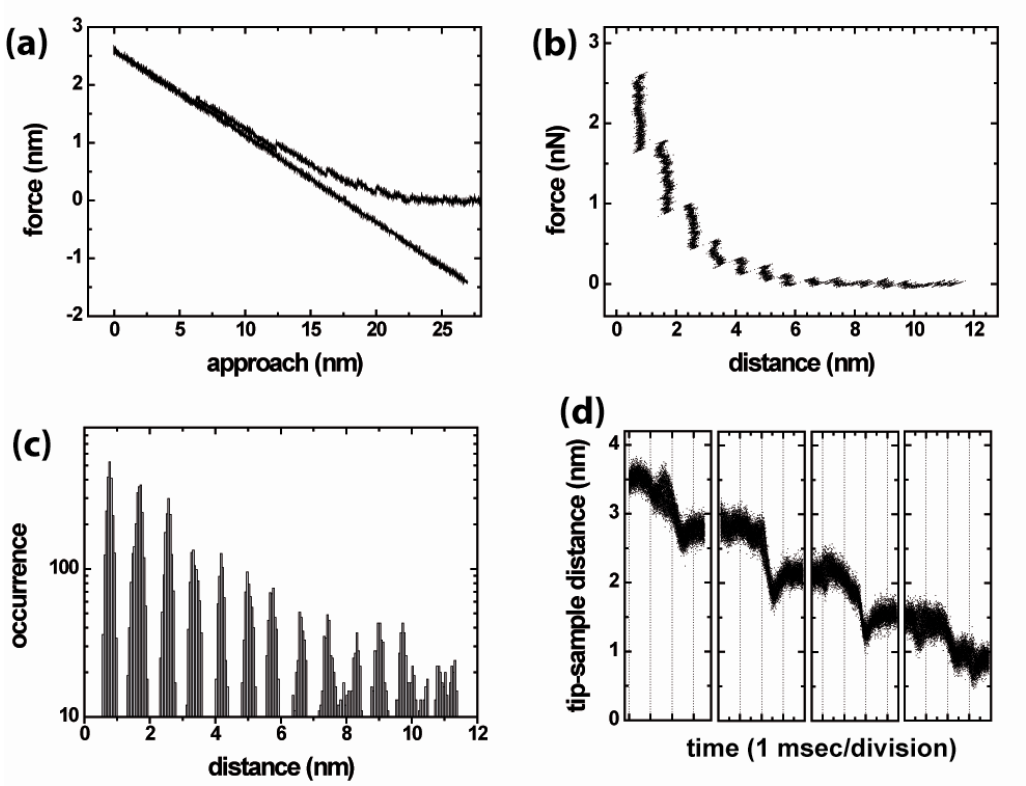

Figure 1: (a) Normal force curve recorded during sample approach in the ionic liquid [Py1,4][FAP], the surface potential is -2V and the approach rate 12 nm/s. The increase of repulsive force is interrupted by several discontinuities, which we attribute to jumps between branches of a oscillatory force which originates in molecular double layers of the ionic liquid. Adhesion leads to an increasing attractive force upon retraction of the sample. (b) Normal force plotted versus the tip-sample distance for the data set presented in (a). The tip-sample distance has been determined as the difference between approach distance and the cantilever deflection. (c) Histogram of distance values in (b), i.e. of a single approach curve. Up to twelve distance plateaus can be recognized, reflecting the layered structure of the ionic liquid as far as 9.5 nm from the surface. The probability to find the tip in a certain distance plateau increases exponentially with decreasing distance. (d) Four jumps in the tip-sample distance from five to one double layer of ionic liquid which have been recorded with high temporal resolution.

A more accessible presentation of the same data is provided by plotting the force vs. the tip-sample distance in figure 1(b). The tip-sample distance has been calculated as the difference between approach distance and cantilever deflection. The precision in calibration of the cantilever deflection is limited by finite stiffness of tip and sample and by non-linear characteristics of the piezo actuators. We estimate that the tip-sample distance is correct within 10%. The distance between each two jump events can be read from the histogram of distance values in figures 1 (c). The average difference between peaks in the histogram is 0.828±0.005 nm, a value still affected by the uncertainty in calibration of the cantilever deflection of 10%. Within this error the jump distance corresponds to a little less than the sum of ionic radii for cation and anion of 0.9 nm derived from bulk density [10]. The ionic liquid [$Py_{1,4}$][FAP] exhibits a particularly long range of layer ordering in front of the Au(111) surface at the potential of -2V. Up to twelve peaks can be recognized in the histogram. The

number of occurrences of each distance plateau increases exponentially as the tip jumps from layer to layer towards the surface.

Force vs. distance experiments performed by AFM do not allow for an independent experimental determination of the distance from surface contact in figures 1(b) and (c). We have chosen to define the position of the last distance plateau in figure 1(b) to be one double layer of anion and cation from the surface since we have experimental evidence that such double layer is still confined between tip and surface. Upon further increase of the force the tip will penetrate the next anion layer, as we will show in the next section in figure 2. The last anion layer can only be penetrated at more positive potential of -1.3 V, resulting in direct contact with the Au(111) surface as described in Ref. [24].

We have also recorded force vs. approach curves with high temporal resolution. Details for four jumps in the cantilever deflection are plotted in figure 1(d). These jumps in the tip-sample distance typically occur on a time scale of 0.2-0.5 milliseconds. The shortest possible reaction time of the cantilever is limited by inertia to about $1/(2\pi*14\ \text{kHz}) = 0.01$ milliseconds assuming a critically damped first flexural bending mode. The time-resolved results exhibit no jumps back and forth between distance plateaus during the transition. Rapid jumps between two distance plateaus have sometimes been observed during similar experiments in the non-polar liquid OMCTS [24].

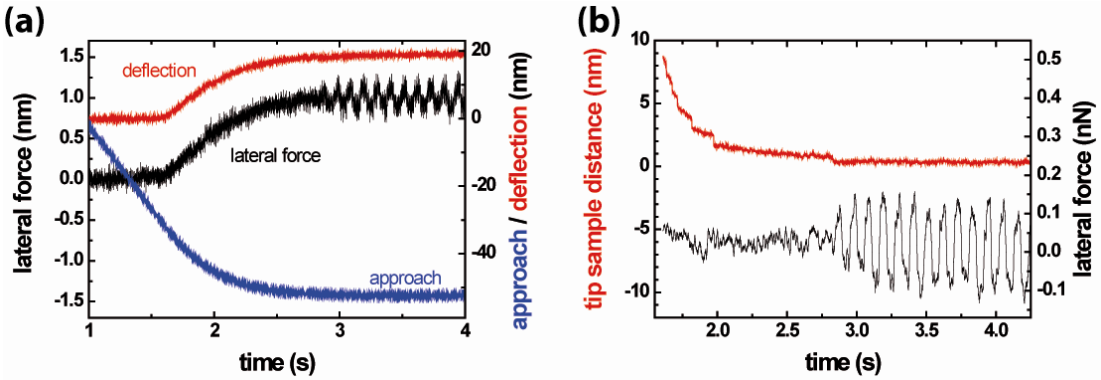

Figure 2 (a) Results of a friction vs. approach experiment as described in the section on experiments. The tip scans a lateral range of 17.5 nm at a rate of 9.6 Hz during the approach. We record the normal deflection (red curve) during the approach. In the deflection signal, the same jumps are observed as in Fig. 1. The approach of the cantilever base position is plotted as blue curve for reference. The black curve reports the lateral force acting on the tip as indicated by the torsional bending of the cantilever. Part of the lateral force signal is cross-talk from the normal force signal, most probably due to a misalignment of cantilever and position-sensitive photodiode. (b) Analysis of the data presented in (a). The cantilever deflection has been converted into the tip-sample distance by subtracting the approach distance. In this experiment, the approach distance is an exponential function of time whose time constant is determined by the feedback settings. The lateral force curve has been corrected for cross-talk by subtracting a multiple of the deflection curve, and has been smoothed using a window of 29 points corresponding to 12 milliseconds.

Friction during approach

A result for the friction vs. approach experiments as described in the experimental section is presented in figure 2. The original data for approach, cantilever deflection, and lateral force is plotted versus time in figure 2(a), the relevant quantities tip-sample distance and lateral force are extracted in figure

2(b). Very similar to the results in figure 1, five jumps in the tip-sample distance of 0.8 nm are observed while the normal force increases over time. However, at t=2.7s the increasing force initiates an additional jump in the tip-sample distance of only 0.45 nm. This last jump indicates the penetration of the last anion layer while the last cation layer remains below the tip apex bound to the surface [24]. At the same time, the lateral force signal starts to exhibit a clear difference in signal between forward and backward motion of the tip. The corresponding friction force is of the order of 100 pN.

Modeling and Discussion

We interpret the results for the force versus distance experiments within a Hertzian contact model, in which the two surfaces interact not only through hard-wall repulsion but also with a finite-range potential. The latter summarizes the effective interaction between the tip and substrate surface that is mediated by the ionic liquid confined between the surfaces. A similar model has been used recently to describe the contact mechanics in the presence of a strongly wetting fluid and to investigate the role of the Tabor coefficient in the case of negative work of adhesion [25].

For the surface energy density $v_{\mathrm{int}}(g)$ between parallel surfaces separated by an interfacial gap g, we assume the following functional dependence:

$$v_{\mathrm{int}}(g) = v_0 \cos\left(\frac{2\pi g}{d}\right) \exp\left(-\frac{g}{\lambda_0}\right) + v_1 \exp\left(-\frac{g}{\lambda_1}\right) \qquad (1)$$

The parameters v_i and λ_i (with i = 0,1) are surface energies and correlation lengths, respectively, and d represents the width of a double layer in the fluid. As we explain in the following paragraph, the first summand on the r.h.s. of Eq. (1) is the dominant far-field term, while the second summand is a correction that only becomes important at short distances.

The functional form of Eq. (1) can be motivated from a pioneering work by Fisher and Widom [26]. Using a model in which atoms interact only with short-range forces, they found that the asymptotic, i.e., long-distance pair correlation function in liquids is described by a single correlation length that is complex at high pressure and real at low pressure. This result implies a monotonically decaying density correlation at low pressure and an oscillatory decay at large pressure, at least in the asymptotic limit. The line in the pT phase diagram separating these two regimes is now known as Fisher-Widom line. For our conditions, the ionic liquid is clearly in the high-density liquid state so that it lies above the Fisher-Widom line and its far-field density correlation function is oscillatory.

Assuming the first fluid layer to have a well-defined distance from each solid wall - which is given by the direct interactions between the fluid and solid atoms - a fluid above the Fisher-Widom line favors separations between two flat solids such that the two outermost fluid layers wetting the surface are accommodated by an integer multiple of the oscillation period. Thus, the oscillations in the pair correlation functions translate into effective interactions between two confining walls that can be described as damped oscillations for sufficiently high fluid densities.

The just-described Fisher-Widom picture remains valid when assuming long-range Coulomb interactions in a binary mixture [27]. Due to electrostatic screening, the asymptotic functional form of the pair-correlation remains unchanged from that for short-range interactions and both charge types are characterized by the same complex correlation length. No van der Waals term is included because the screened van der Waals interaction with the sharp tip is too small to be measured within the stronger correlation forces. A model specific to the ionic liquid would require computer simulations of its density at electrochemical interfaces [21], which are beyond the scope of this study.

We introduce the second term on the r.h.s. of Eq. (1) as the leading-order correction to the Fisher-Widom picture, just like one would add a q^4 term to the phonon dispersion relation $\omega^2 = c^2 q^2$ for

short wavelength excitations of discrete systems. As such, the v_1 term can also be interpreted as a discretization correction. It starts to become important at the point at which the far-field correlation description is no longer accurate. As we discuss further below when presenting our results, we find the second term to be negligible if two or more double layers are sandwiched between tip and substrate.

For curved surfaces, the total (finite-range) interaction energy V_{int} is obtained by integration

$$V_{\mathrm{int}} = \int d^2 r v_{\mathrm{int}}[g(\vec{r})], \qquad (2)$$

where

$$g(\vec{r}) = g_0 + \frac{r^2}{2R_{\mathrm{c}}} - u(\vec{r}). \qquad (3)$$

The gap g_0 between surface and non-deformed tip apex corresponds to the tip-sample distance in figure 1(b), R_c denotes the radius of curvature of the tip apex and $u(\vec{r})$ is the combined elastic displacement of tip and substrate. The center-of-mass mode is gauged such that the mean value of $u_0 = \langle u(\vec{r}) \rangle$ is defined to be zero for a non-deformed tip touching the non-deformed surface in one point.

Inserting Eqs. (3) and (1) for an non-deformed tip-substrate system, for which $g(\vec{r}) = g_0 + r^2/(2R_c)$, into Eq. (2) and substituting $x = r/\sqrt{\lambda R_c}$ yields

$$V_{\mathrm{int}} = V_{\mathrm{int},0} + V_{\mathrm{int},1} \qquad (4)$$

with

$$V_{\mathrm{int},0} = 2\pi v_0 R_{\mathrm{c}} \lambda_0 \exp\left(-\frac{g_0}{\lambda_0}\right) \int_0^\infty dx\, x \cos\left\{2\pi\left(\frac{g_0}{d} + \frac{\lambda_0}{2d}x^2\right)\right\} \exp\left(-\frac{x^2}{2}\right) \qquad (5)$$

and

$$V_{\mathrm{int},1} = 2\pi v_1 R_{\mathrm{c}} \lambda_1 \exp\left(-\frac{g_0}{\lambda_1}\right) \qquad (6)$$

Thus, as is known since Derjaguin's work [28], the interaction potential and thus surface forces are proportional to a product of the form $R_{\mathrm{c}} v_i$ for Hertzian contact geometries. The reason is that R_c only appears as a pre-factor in Eqs. (5) and (6) for any interaction of the form $v_{\mathrm{int}}(g)$, in which gradient corrections are neglected.

Although the integral in Eq. (5) has an analytical solution in terms of error functions with complex arguments, we abstain from writing it down, as it does not further help the analysis of the results. Instead, we content ourselves with noting that $V_{\mathrm{int}}(g_0)$ is a function that decays in the far-field exponentially with g_0 while having a pre-factor periodic in *d*.

The elastic deformation and thus elastic energy V_{ela} is incorporated as

$$V_{\mathrm{ela}}[u(\vec{r})] = \frac{AE^*}{4} \sum_q |\tilde{u}(\vec{q})|^2 \qquad (7),$$

where *E** is the effective modulus, *A* the area of integration and $\tilde{u}(\vec{q})$ the Fourier transform of the displacement field. The total energy, which needs to be minimized with respect to the displacement field, then reads

$$V = -F_{\mathrm{N}} u_0 + V_{\mathrm{ela}} + V_{\mathrm{hw}} + V_{\mathrm{int}} \qquad (8).$$

Here, F_N is the normal load and V_{hw} formally denotes the hard-wall interaction or non-overlap constraint, i.e., $V_{hw} = 0$ when the two surfaces do not touch and $V_{hw} = \infty$ when tip and substrate overlap.

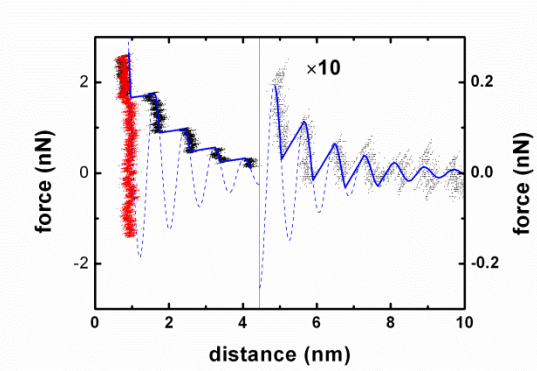

Figure 3 Comparison of data from figure 1 with a model in which the potential is calculated as integral over the tip-sample gap area of exponentially decaying oscillatory contributions (see text for details). The dashed blue line shows the model force curve, the solid blue line the expected force-distance approach curve for the cantilever stiffness of k = 0.15 N/m, and the dots are experimental data points, black dots for approach and red dots for retraction.

The parameters of the model have been adjusted to fit to the experimental data of figure 1; the result is presented in figure The model predicts an oscillatory force curve of exponentially increasing amplitude with decreasing tip-sample distance, with multiple possible distance values for a given normal force. Upon approach, the tip remains on each distance plateau until the increasing normal force reaches the respective maximum of the force curve and a jump to the next branch of the force curve is initiated. Each jump in distance comes with a small drop in force due to the finite stiffness of the cantilever. Positions and force values of the jumps are well reproduced by the model force curve. The model also explains characteristic details in the shape of the experimental force curve, such as the increasing length and the increasing slope of the distance plateaus with decreasing distance. This characteristic details are found in figure 1, but also in results reported by other authors for ionic liquids (for example figure 1 in Ref. [10]) and for non-ionic liquids (for example figure 2 in Ref. [29]).

Such layering was observed in surface forces apparatus (SFA) experiments since the pioneering work by Horn and Israelachvili [30, 31] who found that structural forces cause a layered ordering of octamethylcyclotetrasiloxane (OMCTS) when confined within a SFA. Christenson et al. extended this work to alkanes demonstrating that even these simple liquids show a pronounced layered structure in confinement [32]. In all cases the authors described the oscillatory force profile as a result of mechanical instabilities occurring when gradient of the force exceeds the spring constant.

The process is reminiscent of the atomic stick-slip processes described for friction of nanometer-scale contacts on crystalline surfaces. Atomic slip events occur when the slope of the surface force curve becomes larger than the stiffness of the cantilever [33]. In figure 3, this condition is met for all distance plateaus at distances 8 nm or less, for the plateaus at 8.8 nm and higher the position of the tip still samples the shape of the potentials, but no instabilities occur at the transition from on plateau to the next. Similar to atomic friction experiments, significant amounts of energy are dissipated only when instabilities occur as they result in an adhesion hysteresis when the tip is retracted. Note that the purely repulsive force regime upon approach is only due to the compliance of the cantilever. A much stiffer cantilever would sample both repulsive and attractive parts of the correlation forces, at the

prohibitive cost of much lower sensitivity. SFA experiments often provide higher stiffness with respect to the curvature of the potential, and sample more of the attractive parts of the oscillatory force curves [12, 31, 32].

Table 1 Parameters for the model force curves in figure 3 and figure 5.

	d (nm)	v_0R_c ($J/m^2 \times nm$)	λ_0 (nm)	v_1R_c ($J/m^2 \times nm$)	λ_1 (nm)
figure 3	0.810	0.77	1.51	2.7	0.3
figure 5	0.775	0.82	1.51	2.7	0.3

The parameters for the force curve in figure 3 are provided in table 1. The combined value of the short-distance and far-field surface energies at a distance of one double layer $v_0\exp(-d/\lambda_0) + v_1\exp(-d/\lambda_1)$ is about 70 mJ/m^2 assuming a typical tip radius of R_c=10 nm. The energy is comparable to the typical value expected for attractive van der Waals adhesion energies in contact. The negative adhesion energy due to correlation forces dominating over typical van der Waals attraction at the distance of one double layer is in agreement with the observation that double layers of ionic liquids prevent the snapping of the tip into contact. The value of v_0R_c certainly depends on experimental parameters. Comparison with previously reported studies indicates that v_0R_c increases with increasing electrochemical potential [8, 10], and generally decreases with increasing temperature [7, 29].

The decay length of the 1.51 nm for the correlation interaction is in overall agreement with the characteristic decay length of oscillatory forces which can be read from the respective figures in reports for AFM [8], colloidal probe AFM [10], and SFA experiments [11, 12] in ionic liquids. Note the short range of the correction term v_1 which is limited to the first two distance plateaus. The parameters for the oscillatory far-field interaction v_0 are fully determined by the forces and distances of the other plateaus.

The numerical results reveal at what gaps the experimental results are consistent with a far-field-based picture and at what point it breaks down. As a rough estimate, one could argue that the far-field picture is accurate, at least for the property under scrutiny, as long as the forces associated with the far-field term, i.e. the first one on the r.h.s. of Eq. (1), is more than ten times larger than the corrections. For the parameters listed in Tab. 1, this condition is satisfied for $g > 2\text{nm}$. Severe deviations from the far-field picture occur when the correction forces start to dominate the oscillatory forces. For our expressions, this happens at $g < 1\text{nm}$. Thus, when comparing these numbers with the experimental data, one could argue that we measure predominantly fluid properties down to two double layers within this interpretation. Such an interpretation is in contrast to the occasionally discussed point of view that layering implies solidification.

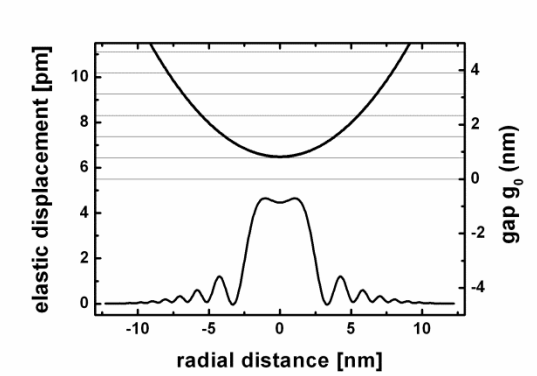

Figure 4: Combined elastic displacement $g(r) - g_0 - r^2/R_c$ of tip and surface for one double layer of ionic liquid confined between tip and surface and a normal force of 2 nN. The upper part of the graph shows the gap $g(r)$ for comparison. The lines indicate the distance between double layers of ionic liquid.

In the present work, tips are relatively rigid with E^*= 125 GPa for the combination of SiO_2 tip and gold substrate. Noticeable deformation occurs only if the closest distance between tip and substrate is one monolayer or less. As an example, we have calculated the combined displacement of tip and sample for a situation where one double layer of ionic liquid is confined between a tip of R_c=10 nm radius with an applied normal force of 2 nN. The deformation is plotted as a function of the radial distance in figure 4. The deformations at the tip apex are of the order of a few picometers, negligible in comparison to the gap width. The decaying oscillations of the elastic deformation as function of the radial distance illustrate the contributions of different thickness of the liquid layer due to the curvature of the tip. Based on these results of negligible elastic deformation, we have not taken into account the deformation terms whenever we have modeled approaches to distances $g_0 > d$ larger than the last double layer.

The observed number of up to 12 layers in the force vs. approach curves is higher than in most other colloidal probe AFM or SFA experiments. Since our experiments employ some of the sharpest tips commercially available, we speculate that the tip sharpness plays a role for the number of observed layers. This assumption is in agreement with the early observations that solvation shells in water are best detected by either SFA with an almost parallel surface configuration or by the sharpest tip available, a carbon nanotube [34]. Any roughness at the probe apex will wash out the influence of layering on the force curves, and both very sharp AFM tips and the atomically smooth mica sheets in SFA experiments can be regarded as low-roughness probes.

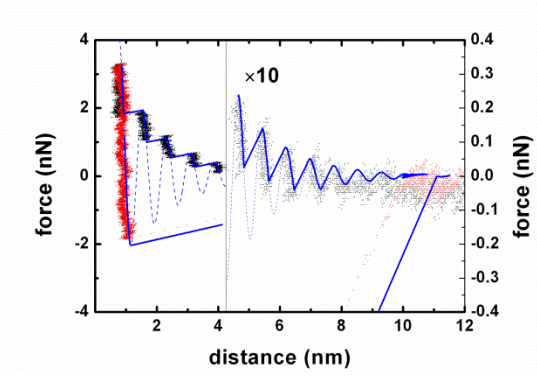

Figure 5: Comparison of force vs tip-sample distance data recorded with a different cantilever of lower stiffness, the surface potential is -2V and the approach rate 12 nm/s.

The dashed blue line shows the model force curve, the solid blue line the expected force-distance approach curve for the cantilever stiffness of k = 0.21 N/m, and the dots are experimental data points, black dots for approach and red dots for retraction. Upon retracting the tip jumps away from the distance plateau closest to the surface at the negative normal force predicted by the model.

A second set of force vs. tip-sample distance data, recorded with a slightly stiffer cantilever in $[Py_{1,4}][FAP]$ over the Au(111) surface at -2 V potential is presented together with the respective model force curve in figure 5. In this case, the negative normal force upon retraction was strong enough to initiate a jump back from the distance of the last double layer. Force and position of the jump are closely predicted by the model. The experimental force curve during the jump back does not intersect with any of the first twelve force peaks and, therefore, no layering is observed upon retraction. The parameters used for the model force curve are given in Tab. 1, differences to the parameters for the results in figure 3 indicate the overall precision of the experiments and their analysis. Similar results for adhesive forces upon retraction of the tip and subsequent jumps over several double layers have been reported for different ionic liquids (EAN in Ref. [14] or BMIPF6 in Ref. [8]). The results in these reports can be fully described within the framework of our proposed model along the interpretation of the data in figure 5.

The jump of the tip through each double layer of ionic liquid upon approach takes several tenths of a millisecond, an order of magnitude longer than the characteristic reaction time of the force sensor (see figure 1(d)). Similarly, the overshoot observed after most jumps takes too long to be the result of cantilever inertia alone. We conclude that the time scale of these processes reflects the time required to establish the correlation order in the tip-sample confinement. It can be thought of a time scale of the nanometer-scale viscosity of the system.

Finally, we discuss the frictional response upon approach to the surface. When we approach the tip to the surface while scanning it back and forth laterally, we still see the jumps in the normal cantilever deflection indicating the layering forces of the double layers. We do not see any friction until the last anion layer is penetrated, in agreement with our recent result for the same system [24]. The absence of friction beyond the last ionic layer is in contrast to colloidal probe AFM results for the ionic liquid ethyl ammonium nitrate (EAN) on mica [14] and to SFA results for the ionic liquid $[Py_{1,4}][Tf_2N]$ with the anion bis[(trifluoromethane)sulfonyl] imide on mica [15]. One could assume that the Derjaguin approximation [28] for normal forces is also valid for lateral forces and shear stress across all length scales. Under this assumption, we can compare the different results using a scaling of lateral force divided by the tip radius. Smith et al. reported lateral forces of the order of F=40 µN in the layering regime with a tip radius of about R=10 mm [15]. With a tip of 10 nm radius we would expected lateral forces of about 40 pN, just within the sensitivity of our current experiment. The continuously increasing friction forces recorded by Werzer et al. with a colloidal probe AFM when approaching through four double layers of the ionic liquid do not show any signature of the layering [14]. Their friction values of < 0.5 nN acting on the colloidal probe with 10 µm radius would be below our detection limit if the scaling law applies.

The results by Werzer et al. [14] and by Smith et al. [15] have been obtained for mica, a surface with strong lateral variation of the atomic-scale electrostatic potential. This spatially varying electrostatic surface potential may perturb the fluid structure, even pin the ionic liquid to the mica surface, and cause the observed friction on pinned layers of ionic liquids. In the case of the Au(111) surface, only high normal pressures will lead to an interlocking of tip, molecules, and surface and result in significant friction [35, 36]. One also has to keep in mind that in SFA experiments the confinement of the ionic liquid to a few nanometers extends laterally over an area which is several orders of

magnitude larger than in AFM experiments. This extreme geometry may contribute to collective dynamics in the confined liquid which lead to friction.

Conclusions

The layering of the ionic liquid $[Py_{1,4}][FAP]$ in the confinement between an AFM tip and a Au(111) surface at an electrochemical potential of -2V extends as far as twelve pairs of anion and cation layers, as detected by jumps in the force curves recorded during approach of the tip to the surface. The jumps are interpreted as instabilities which occur when the soft cantilever spring probes an oscillatory force with exponentially increasing amplitude. The far-field potential can be derived from a single complex correlation length, which is consistent with the long-range picture of correlations in a fluid from density correlations of the ionic liquid. Its characteristic decay length λ and oscillation periodicity d ($\lambda \cong 1.5$ nm and $d \cong 0.8$ nm for $[Py_{1,4}][FAP]$) depend only on the respective correlated interactions in the liquid and not on the curvature of the probing surfaces. To explain the jumps in the tip-sample distance, this interpretation does not require any solidification or squeeze-out mechanisms which have been occasionally suggested in the interpretation of AFM experiments. The instabilities rather resemble the atomic stick-slip mechanism known from friction experiments on crystalline surfaces, where the oscillating lateral potential and a compliant force sensor lead to the stick-slip motion. The adhesion hysteresis measured by AFM in ionic liquids depends therefore critically on the stiffness of the probing force sensor.

Friction between the approaching AFM tip and the Au(111) surface mediated by the ionic liquid was found to be below the detection limit of the current set up, until the tip reached the last cation layer, which is bound to the negatively charged surface. The absence of friction in the ionic liquid despite the observation of oscillatory normal forces supports our picture for $[Py_{1,4}][FAP]$ on Au(111) as a liquid with nanometer-range correlations, but without any signatures of solidification beyond the first cation layer.

Acknowledgements

Authors at the INM thank Eduard Arzt for continuous support of the project. The ionic liquid sample has been generously provided by Frank Endres, University Clausthal-Zellerfeld. The project has been financially supported by the Volkswagen-Stiftung.

References

[1] Bermúdez M-D, Jiménez A-E, Sanes J and Carrión F-J 2009 Ionic Liquids as Advanced Lubricant Fluids *Molecules* **14** 2888-908

[2] Minami I 2009 Ionic Liquids in Tribology *Molecules* **14** 2286-305

[3] Predel T, Pohrer B and Schlücker E 2010 Ionic Liquids as Alternative Lubricants for Special Applications *Chemical Engineering & Technology* **33** 132-6

[4] Zhou F, Liang Y and Liu W 2009 Ionic liquid lubricants: designed chemistry for engineering applications *Chemical Society Reviews* **38** 2590-9

[5] Mezger M, Schroder H, Reichert H, Schramm S, Okasinski J S, Schoder S, Honkimaki V, Deutsch M, Ocko B M, Ralston J, Rohwerder M, Stratmann M and Dosch H 2008 Molecular layering of fluorinated ionic liquids at a charged sapphire (0001) surface *Science* **322** 424-8

[6] Atkin R and Warr G G 2007 Structure in confined room-temperature ionic liquids *Journal of Physical Chemistry C* **111** 5162-8

[7] Hayes R, Warr G G and Atkin R 2010 At the interface: solvation and designing ionic liquids *Physical Chemistry Chemical Physics* **12** 1709

[8] Zhang X, Zhong Y-X, Yan J-W, Su Y-Z, Zhang M and Mao B-W 2012 Probing double layer structures of Au (111)-BMIPF6 ionic liquid interfaces from potential-dependent AFM force curves *Chemical Communications* **48** 582-4

[9] Li H, Endres F and Atkin R 2013 Effect of alkyl chain length and anion species on the interfacial nanostructure of ionic liquids at the Au(111)-ionic liquid interface as a function of potential *Physical Chemistry Chemical Physics* **15** 14624-33

[10] Hayes R, Borisenko N, Tam M K, Howlett P C, Endres F and Atkin R 2011 Double Layer Structure of Ionic Liquids at the Au(111) Electrode Interface: An Atomic Force Microscopy Investigation *The Journal of Physical Chemistry C* **115** 6855-63

[11] Bou-Malham I and Bureau L 2010 Nanoconfined ionic liquids: effect of surface charges on flow and molecular layering *Soft Matter* **6** 4062

[12] Perkin S 2012 Ionic liquids in confined geometries *Physical Chemistry Chemical Physics* **14** 5052-62

[13] Perkin S, Crowhurst L, Niedermeyer H, Welton T, Smith A M and Gosvami N N 2011 Self-assembly in the electrical double layer of ionic liquids *Chemical Communications* **47** 6572-4

[14] Werzer O, Cranston E D, Warr G G, Atkin R and Rutland M W 2012 Ionic liquid nanotribology: mica-silica interactions in ethylammonium nitrate *Physical Chemistry Chemical Physics*

[15] Smith A M, Lovelock K R J, Gosvami N N, Welton T and Perkin S 2013 Quantized friction across ionic liquid thin films *Physical Chemistry Chemical Physics* **15** 15317-20

[16] Sweeney J, Hausen F, Hayes R, Webber G B, Endres F, Rutland M W, Bennewitz R and Atkin R 2012 Control of Nanoscale Friction on Gold in an Ionic Liquid by a Potential-Dependent Ionic Lubricant Layer *Physical Review Letters* **109**

[17] Li H, Rutland M W and Atkin R 2013 Ionic liquid lubrication: influence of ion structure, surface potential and sliding velocity *Physical Chemistry Chemical Physics* **15** 14616-23

[18] Lanning O J and Madden P A 2004 Screening at a charged surface by a molten salt *J. Phys. Chem. B* **108** 11069-72

[19] Pinilla C, Del Popolo M G, Lynden-Bell R M and Kohanoff J 2005 Structure and dynamics of a confined ionic liquid. topics of relevance to dye-sensitized solar cells *J. Phys. Chem. B* **109** 17922-7

[20] Kirchner K, Kirchner T, Ivaništšev V and Fedorov M V 2013 Electrical double layer in ionic liquids: Structural transitions from multilayer to monolayer structure at the interface *Electrochimica Acta* **110** 762-71

[21] Merlet C, Rotenberg B, Madden P A and Salanne M 2013 Computer simulations of ionic liquids at electrochemical interfaces *Physical Chemistry Chemical Physics* **15** 15781-92

[22] Ueno K, Kasuya M, Watanabe M, Mizukami M and Kurihara K 2010 Resonance shear measurement of nanoconfined ionic liquids *Physical Chemistry Chemical Physics* **12** 4066-71

[23] Green C, Lioe H, Cleveland J, Proksch R, Mulvaney P and Sader J 2004 Normal and torsional spring constants of atomic force microscope cantilevers *Rev. Sci. Instrum.* **75** 1988-96

[24] Sweeney J, Hausen F, Hayes R, Webber G B, Endres F, Rutland M W, Bennewitz R and Atkin R 2012 Control of Nanoscale Friction on Gold in an Ionic Liquid by a Potential-Dependent Ionic Lubricant Layer *Phys. Rev. Lett.* **109** 155502

[25] Müser M H 2013 On single-asperity contact mechanics with positive and negative work of adhesion *Beilstein Journal of Nanotechnology* **submitted**

[26] Fisher M E and Wiodm B 1969 Decay of Correlations in Linear Systems *The Journal of Chemical Physics* **50** 3756-72

[27] Leote de Carvalho R J F and Evans R 1994 The decay of correlations in ionic fluids *Molecular Physics* **83** 619-54

[28] Derjaguin B 1934 Untersuchungen über die Reibung und Adhäsion, IV *Kolloid-Zeitschrift* **69** 155-64

[29] de Beer S, Wennink P, van der Weide-Grevelink M and Mugele F 2010 Do Epitaxy and Temperature Affect Oscillatory Solvation Forces? *Langmuir* **26** 13245-50

[30] Horn R G and Israelachvili J N 1980 DIRECT MEASUREMENT OF FORCES DUE TO SOLVENT STRUCTURE *Chemical Physics Letters* **71** 192-4

[31] Horn R G and Israelachvili J N 1981 DIRECT MEASUREMENT OF STRUCTURAL FORCES BETWEEN 2 SURFACES IN A NON-POLAR LIQUID *J. Chem. Phys.* **75** 1400-11

[32] Christenson H K, Gruen D W R, Horn R G and Israelachvili J N 1987 STRUCTURING IN LIQUID ALKANES BETWEEN SOLID-SURFACES - FORCE MEASUREMENTS AND MEAN-FIELD THEORY *J. Chem. Phys.* **87** 1834-41

[33] Socoliuc A, Bennewitz R, Gnecco E and Meyer E 2004 Transition from stick-slip to continuous sliding in atomic friction: Entering a new regime of ultralow friction *Phys. Rev. Lett.* **92**

[34] Jarvis S P, Uchihashi T, Ishida T, Tokumoto H and Nakayama Y 2000 Local solvation shell measurement in water using a carbon nanotube probe *J. Phys. Chem. B* **104** 6091-4

[35] He G, Muser M H and Robbins M O 1999 Adsorbed layers and the origin of static friction *Science* **284** 1650-2

[36] Müser M H, Wenning L and Robbins M O 2001 Simple Microscopic Theory of Amontons's Laws for Static Friction *Phys. Rev. Lett.* **86** 1295-8